Supporting Information

Synergistic engineering of atomic disorder and porous architectures for ultralow lattice thermal conductivity and enhanced thermoelectric performance in n-type high-entropy lead chalcogenides

Qian Deng, [a] Xiaobo Tan, [a] Ruiheng Li, [a] Yin Xie, [a] Zhilong Zhao, [a] Jiaxing Luo, [a] and Ran Ang*[a,b,c]

[a]Key Laboratory of Radiation Physics and Technology, Ministry of Education, Institute of Nuclear Science and Technology, Sichuan University, Chengdu 610064, China

[b]College of Physics, Sichuan University, Chengdu 610064, China

[c]Institute of New Energy and Low-Carbon Technology, Sichuan University, Chengdu 610065, China

*Corresponding author and Email: rang@scu.edu.cn

Electrical transport modeling

The density of state effective mass m^* and Lorenz number L were calculated based on single Kane band (SKB) model by the following equations:[1]

Seebeck coefficient

$$S = \frac{k_b}{e}\left[\frac{{}^{1}_{0}F^{1}_{-2}}{{}^{0}_{0}F^{1}_{-2}} - \xi\right] \qquad \text{(eq. S1)}$$

Hall carrier density

$$n_H = \frac{1}{A}\left[\frac{2m^* k_B T}{\hbar^2}\right]^{3/2} {}^{0}_{0}F^{2/3}_{0} \qquad \text{(eq. S2)}$$

Hall factor

$$A = \frac{3K(K+2)\,{}^{0}_{0}F^{1/2}_{-4}\,{}^{0}_{0}F^{2/3}_{0}}{(2K+1)^2\ \left({}^{0}_{0}F^{1}_{-2}\right)^2} \qquad \text{(eq. S3)}$$

Lorenz number

$$L = \frac{\kappa_B^2}{e^2}\left[\frac{{}^{2}_{0}F^{1}_{-2}}{{}^{0}_{0}F^{1}_{-2}} - \left(\frac{{}^{1}_{0}F^{1}_{-2}}{{}^{0}_{0}F^{1}_{-2}}\right)^2\right] \qquad \text{(eq. S4)}$$

Carrier mobility

$$\mu = \frac{2\pi\hbar^4 e C_l \qquad 3\,{}^{0}_{0}F^{1}_{-2}}{m_I^*\,(2m^* k_B T)^{3/2}\,\Xi^2\,{}^{0}_{0}F^{3/2}_{0}} \qquad \text{(eq. S5)}$$

Generalized Fermi integral

$${}^{n}_{0}F^{m}_{l}(\xi,\alpha) = \int_0^\infty \left(-\frac{\partial f}{\partial \varepsilon}\varepsilon^n\right)(\varepsilon + \varepsilon^2\alpha)^m (1 + 2\varepsilon\alpha)^l d\varepsilon \qquad \text{(eq. S6)}$$

Here, k_B is the Boltzmann constant, K is the the anisotropy factor, ${}^{n}_{0}F^{m}_{l}(\xi,\alpha)$ is the generalized Fermi integral, Ξ is the deformation potential of materials, C_l is the average longitudinal elastic

constant, ε is the reduced carrier energy $\varepsilon = E/k_B T$, m^* is effective mass of charge carriers, m_I^* is the inertial effective mass, and the reduced chemical potential is given by $\xi = E_F/(k_B T)$, where E_F is the Fermi energy.

Details of weighted mobility and quality factor calculations

Weighted mobility (μ_w) and quality factor (B) were calculated using the following equations:[2,3]

$$\mu_W = \frac{3\sigma h^2}{8\pi e(2m_e k_B T)^{3/2}}\left[\frac{exp\left[\frac{|S|}{k_B/e}\right]}{1+exp\left[-5\left(\frac{|S|}{k_B/e}-1\right)\right]}+\frac{\frac{3}{\pi^2}\frac{|S|}{k_B/e}}{1+exp\left[5\left(\frac{|S|}{k_B/e}-1\right)\right]}\right] \quad \text{(eq. S7)}$$

$$B = \left(\frac{k_B}{e}\right)^2 \frac{8\pi e(2m_e k_B T)^{3/2}}{3h^2}\frac{\mu_W}{\kappa_{lat}}T \quad \text{(eq. S8)}$$

Supplementary details

Figure S1. Scanning electron microscopy images of (a) pristine PbSe, (b) $PbSe_{0.996}Br_{0.004}$, and (c) $Pb_{0.9}Sn_{0.1}Se_{0.496}Br_{0.004}Te_{0.25}S_{0.25}$.

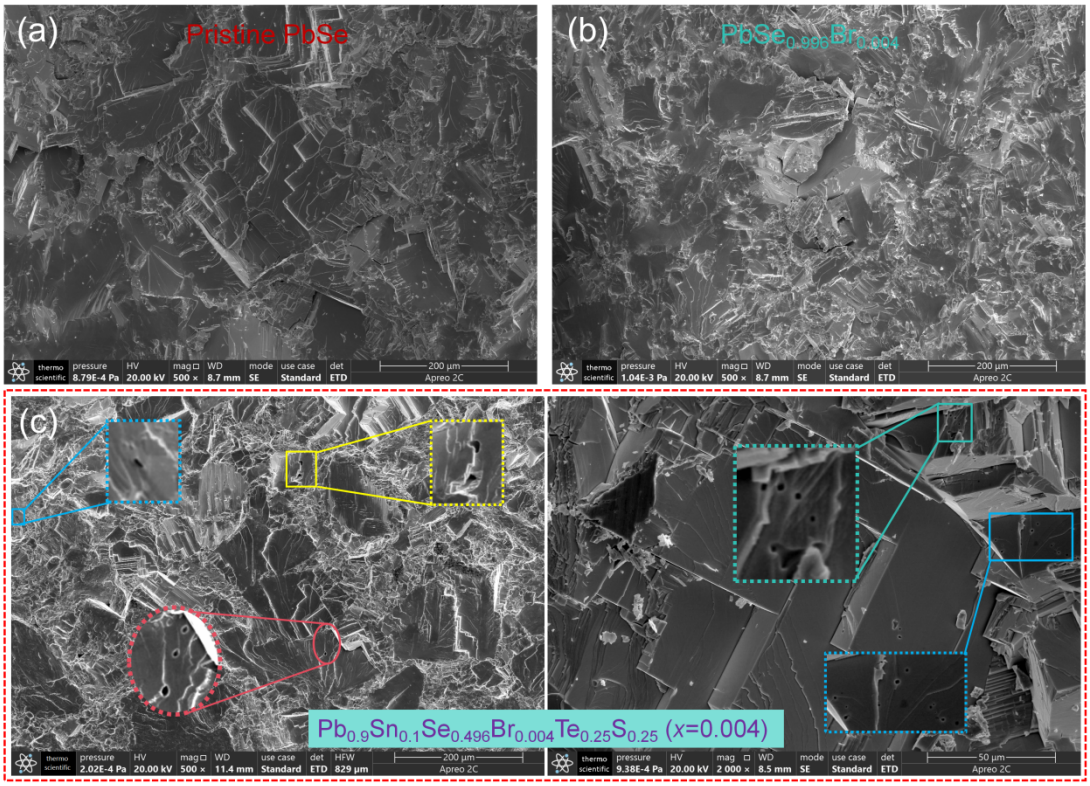

Figure S2. Thermoelectric performance of pristine PbSe. Temperature-dependent (a) electrical conductivity σ, (b) Seebeck coefficient S, (c) total thermal conductivity κ_{tot}, and (d) figure-of-merit zT.

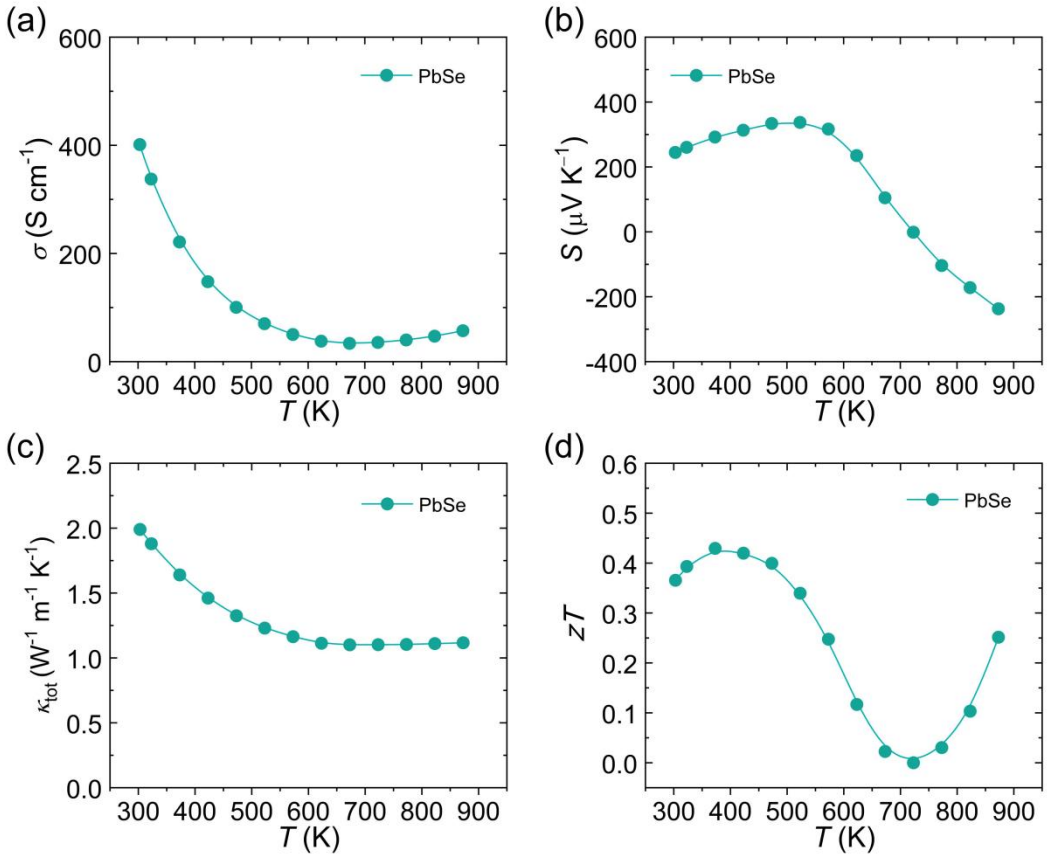

Figure S3. Temperature-dependent lattice thermal conductivity κ_{lat} for pristine PbSe and $Pb_{0.9}Sn_{0.1}Se_{0.5-x}Br_xTe_{0.25}S_{0.25}$ (x = 0.002, 0.003, 0.004, and 0.005).

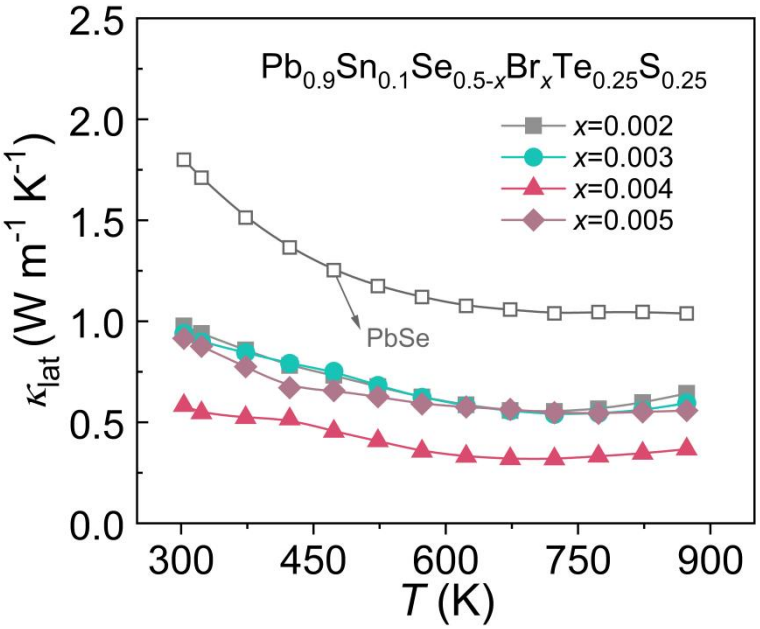

Figure S4. Thermoelectric performance of n-type $PbSe_{0.996}Br_{0.004}$. Temperature-dependent (a) electrical conductivity σ, (b) Seebeck coefficient S, (c) total thermal conductivity κ_{tot}, and (d) figure-of-merit zT.

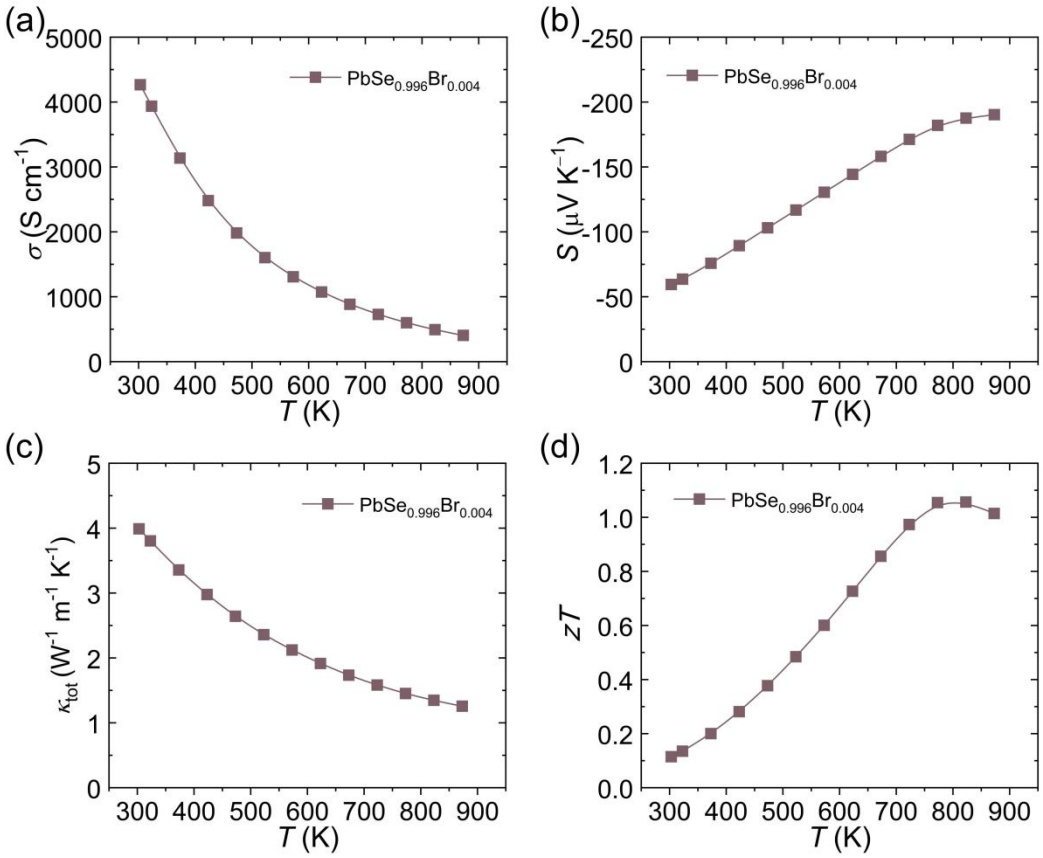

Figure S5. Thermoelectric performance of p-type $(GeTe)_{0.85}(AgSbSeS)_{0.15}$ for the single-stage device construction. Temperature-dependent (a) electrical conductivity σ, (b) Seebeck coefficient S, (c) total thermal conductivity κ_{tot}. (d) Temperature-dependent figure-of-merit zT for n-type $Pb_{0.9}Sn_{0.1}Se_{0.496}Br_{0.004}Te_{0.25}S_{0.25}$ and p-type GeTe-based sample.

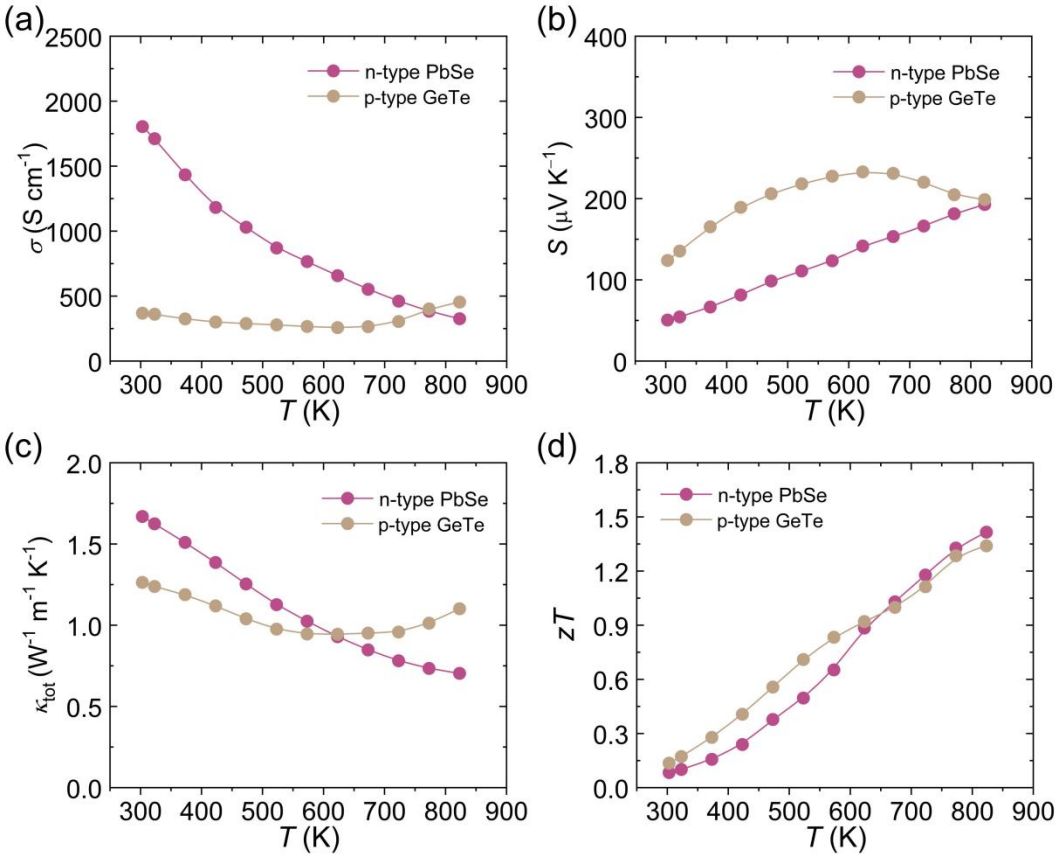

Figure S6. Heat flow (Q) as functions of current (I) for the n-type $Pb_{0.9}Sn_{0.1}Se_{0.496}Br_{0.004}Te_{0.25}S_{0.25}$-based TE device.

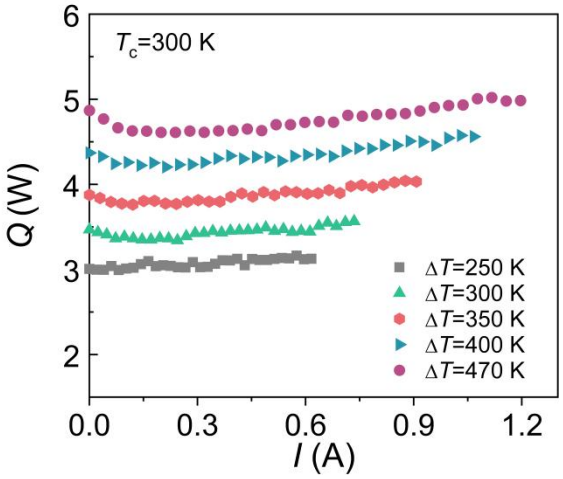

1. E. O. Kane, *J. Phys. Chem. Solids*, 1957, **1**, 249-261.
2. G. J. Snyder, A. H. Snyder, M. Wood, R. Gurunathan, B. H. Snyder and C. N. Niu, *Adv. Mater.*, 2020, **32**, 2001537.
3. Y. Pei, H. Wang and G. J. Snyder, *Adv. Mater.*, 2012, **24**, 6125-6135.